Super-Resolution Fluorescence Optical Microscopy: Targeted and Stochastic Read-Out Approaches

Alberto Diaspro, Francesca Cella Zanacchi, Paolo Bianchini and Giuseppe Vicidomini

Abstract This chapter is dedicated to a general overview of some of the emerging and well-established super-resolution techniques recently developed and known as optical nanoscopy and localization precision method. Due to the way of probing the sample, one can consider them as targeted and stochastic-based techniques, respectively. Here, we stress how super-resolution is obtained without violating any physical law, i.e., diffraction. The strong idea behind such approaches, operating in fluorescence contrast mode, is related to the ability of controlling the states, bright/dark or red/blue, of the fluorescent labels being used in order to circumvent the diffraction barrier. Super-resolution is achieved by precluding simultaneous emission of spectrally identical emission of adjacent (<diffraction limit distance) molecules. Also, the evolution of such techniques toward applications on thick (>50 micron thickness) samples is discussed along with correlative microscopy approaches involving scanning probe methods. Examples are given within the neuroscience framework.

1 Introduction

One of the most relevant optical microscopy approaches toward cell studies, i.e., far-field fluorescence optical microscopy, in the last 30 years benefited of a series of key advances from confocal to multiphoton microscopy [22], from single-molecule detection methods to super-resolution microscopy and optical nanoscopy [23, 24, 41]. Also, advances in labeling techniques, imaging speed, and detection sensitivity greatly expanded the impact of fluorescence optical microscopy in life sciences [66]. Unfortunately, spatial information about packed or adjacent

A. Diaspro (✉) · F. C. Zanacchi · P. Bianchini · G. Vicidomini
NanoBioPhotonics—LAMBS, Nanophysics, Istituto Italiano di Tecnologia, Via Morego 30, 16163 Genoa, Italy
e-mail: alberto.diaspro@iit.it

F. Benfenati et al. (eds.), *Novel Approaches for Single Molecule Activation and Detection*, Advances in Atom and Single Molecule Machines,
DOI: 10.1007/978-3-662-43367-6_3,

(positioned at distances closer than the diffraction limit, i.e., approx. 200 nm) fluorescent molecules—that one should consider as nanoscale sources of light having a size ranging from 1 to 5 nm—is irretrievably lost when the related signatures overlap on a microscopic image [71]. This prevents the ability of following in a quantitative way biological mechanisms molecule by molecule. Such a scenario dramatically changed with the development of a number of methods that are usually grouped as super-resolution optical microscopy approaches. In general, the so-called super-resolution microscopies, realized using focused light, can be separated into two main categories, namely stochastic read-out or localization methods and targeted read-out or engineering point spread function (PSF) methods. However, improvement in spatial resolution is one of the requirements when developing advanced optical methods and should be balanced with others such as low phototoxicity, temporal resolution, penetration depth, and artifacts minimization [73]. As early reported [86], one of the most relevant developments in super-resolution and/or single-molecule detection methods is the one that brings single-molecule observation to the interior of living cells [18]. We would add that a great jump is moving from super-resolution imaging of single cells on glass slides to cell aggregates, organs, and tissues [12, 13, 45]. Specimens are rarely optically transparent, and imaging depth can be hampered by wavefront distortions mainly caused by random scattering and undesired absorption. The basic idea of precluding spectrally identical emitting fluorescent molecules to emit in the very same temporal acquisition window allows circumventing the inherent physical constraint given by the utilization of focusing lenses. Single molecules mapped into an image by an objective lens of numerical aperture NA appear as confused in a unique emission pattern when they are closer than $\lambda\_em/(2NA)$. Likewise, diffraction makes impossible to focus excitation light of wavelength $\lambda\_ex < \lambda\_em$ more sharply than to a spot of $\lambda\_ex/(2NA)$ in size. As a result, features that are spectrally identical and closer than the diffraction limit, say $\lambda/(2NA)$, are difficult to be separated. It turns that part of the modern research in microscopy has been focused to improve spatial resolution and effective far-field optical methods have been designed and implemented to this end (STED/RESOLFT, PALM/STORM and SSIM) [73]. Some of these approaches realize a substantial spatial resolution improvement by precluding simultaneous emission of fluorescent molecules closer than the diffraction limit. Key differences rely on the mechanism by which the fluorescence emission is modulated/controlled and by whether the emission takes place [at specific space coordinates (STED/RESOLFT) or at random coordinates molecule by molecule (PALM, STORM)]. In parallel, new classes of fluorescent dyes and proteins able to selectively target specific molecules in biological samples and suitable for the super-resolution approaches have been developed, becoming an election tool for imaging biological sub-structures at the whole-cell level [30, 44]. Despite the development of brighter and spectrally optimized fluorescent molecules, super-resolution imaging in depth is limited and its application to thicker samples represents one of the most challenging tasks.

2 Toward Super-Resolution Imaging of Thick (>50 Mm) Biological Specimens

Recently, several advances, both in single-molecule localization-based techniques and in stimulated emission depletion (STED) microscopy, brought to a wider application range of super-resolution techniques toward imaging of thick scattering objects [4, 8, 11–13, 27, 50, 55, 59, 83]. Also, comparatively new methods for 3D imaging of large biological samples, such as two-photon excitation (2PE) and selective plane illumination microscopy (SPIM), are now mature for super-resolution completing the framework comprising confocal and computational optical sectioning microscopy [9, 26, 47, 76, 95]. The growing interest in tissue and large organisms imaging has led in the last few years to an increased popularity of fluorescence techniques such as (2PE) microscopy [20] and light-sheet-based microscopy [47]. Nonlinear microscopy is an elegant method, based on the use of nonlinear contrast mechanism [21, 26], to perform non-invasive deep imaging and became in the last decade the election tool for whole organism and tissue imaging. 2PE laser scanning microscopy (LSM) opened a rapidly expanding field of imaging studies in intact tissues and living animals. Two main reasons make 2PE-LSM the matter of choice for deep imaging: First, because for commonly used fluorescent markers, the TPE needs near-infrared light (700–1,000 nm), which not only penetrates deeper into scattering samples but is also less phototoxic; and the second major advantage of 2PE, similarly shared also with all nonlinear contrast mechanisms, is that the signal depends supralinearly on the density of the excitation photons. Thereby, when focusing the laser beam into the sample, the generation of fluorescence signal is spatially confined to the perifocal region, i.e., out-of-focus fluorescent signal, which is intrinsic of one-photon excitation and which is usually rejected by using confocal detection, is not anymore a problem. Further, confinement of the fluorescence is maintained even in strongly scattering sample because the density of scattered excitation photons is too weak to generate TPE. Within this scenario, the use of higher wavelengths and the exploitation of 2PE represent a unbeatable opportunity to improve imaging depth capabilities and performances of far-field super-resolution techniques [8, 12, 13, 27]. STED microscopy has been initially used to image cortical spines in brain slices in depth, and recently, its combination with 2PE represents an optimal opportunity for multicolor imaging in living brain tissue. STED allowed two-color super-resolution imaging in acute brain slices [5] and the study neuronal morphology up to 30-mm deep in living brain tissue [82]. Furthermore, the implementation of adaptive optics has been proven to be a good opportunity to minimize the aberration effects in STED microscopy [35]. 2PE can also be used to improve performances of localization-based techniques through the confinement of the photoactivation process and the higher imaging depth capability provided. On the other side, light-sheet-based fluorescence microscopy has been recently established as one of the most promising tools for live, three-dimensional and fast imaging in depth [47, 49]. In SPIM, a confined illumination volume is used to excite a thin layer

orthogonally oriented to the detection path, thus reducing the phototoxicity and allowing fast 3D imaging of biological samples in depth. Light-sheet-based microscopy has been recently proven to be a golden approach for improving imaging capabilities of entire organisms and tissues, thus improving the imaging depth capabilities and reducing scattering effects due to light–sample interactions [64]. Furthermore, light-sheet-based configurations have been successfully combined with 2PE [12, 13, 65, 88], showing a reduction of the scattering effects and improved imaging performances [52]. Here, the use of particular optical arrangements, such as light-sheet-based illumination [12, 13] and array tomography [63], extended the imaging depth capabilities (up to 150 microms) of single-molecule localization-based techniques in cellular cell spheroids and intact brain tissue, respectively. Furthermore, the use of efficient dyes emitting in the near-infrared range [2], the wide range of laser sources currently available, and the improved sensitivity of the new generation of sensors are also contributing to the extension of the applicability of super-resolution techniques toward tissue and whole-animal imaging.

A different optical microscopy approach, out from the scope of this paper but worth to be mentioned and able to reach sub-diffraction spatial resolution using non-uniform illumination, is represented by structured illumination (SIM). This technique is based on a widefield architecture, and periodic illumination patterns with high spatial frequency are applied to the sample. Images corresponding to different orientation and phases are used to reconstruct a super-resolution image with spatial resolution doubled in the focal plane compared to conventional microscopy [36]. Furthermore, the combination of SIM with fluorescence saturation (SSIM) allowed to push the spatial resolution reachable down to 50 nm in the 2D case [37]. SIM has been used for 3D super-resolution imaging at the cellular level in living samples [38, 72, 75]. SIM-based techniques are a challenging task in thick samples and tissues since the patterned illumination and the wavefronts are strongly affected/degraded in inhomogeneous samples. For this reason, SIM imaging is often restricted to cells or thin sections. Recently, a combination of line scanning and SIM microscopy improved the modulation and the quality of the illumination pattern, allowing optically sectioned images of 30-μm-thick fluorescent sample [57]. On the other side, a recent approach based on multifocal SIM microscopy, allowed three-dimensional (3D) super-resolution in live multicellular organisms [99]. A strong improvement in the maximum imaging depth reachable by SIM (>45 μm) has been obtained thanks to the rejection of out-of-focus light by means of sparse multifocal illumination patterns. This super-resolution technique allowed microtubules imaging in live transgenic zebrafish embryos.

In the next paragraphs, we focus on PALM-like and STED-like methods.

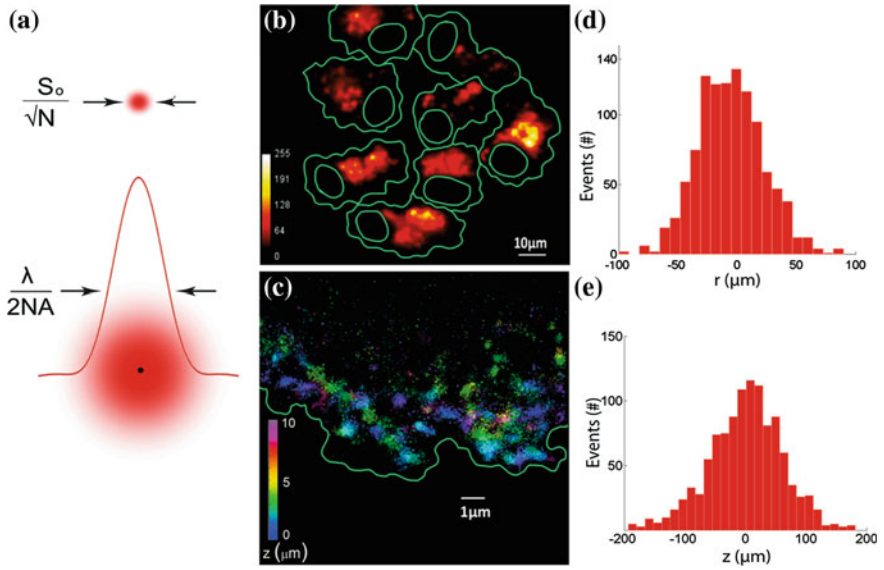

Fig. 1 Schematic representation of the localization process (**a**). Selective plane illumination imaging of the entire mammary cell spheroid (**b**) and super-resolution imaging of connexin43 spatial distribution (**c**) in different planes (*z color-coded map*). The effective localization accuracy estimated directly within thick biological samples in the radial (**d**) and axial (**e**) direction (68 and 141 nm, respectively). (Image modified from [12, 13])

3 Single-Molecule Localization Techniques (Palm-Like)

Detection of single molecules was a pioneering work, carried out more than 20 years ago in condensed phases [58]. The ability to recognize and localize single molecules from pixelated recordings was successful in several cases [6, 10, 16, 17, 31, 51, 85, 96, 97]. When one is confident enough of dealing with a single emitting molecule, then this extra knowledge allows one to interpret the center of the PSF as a measurement of the location of the molecule. Talking about super-resolution, so invoking the ability of discerning to light sources when at distances closer than the diffraction limit, could be risky without a series of "clever" assumptions when forming an image. Within this scenario, in the past few years, several emerging super-resolution techniques, based on localization of single molecules, have been used to provide information of the cellular protein organization with a spatial resolution far beyond the diffraction limit [7, 43, 70]. The basic idea behind these techniques is the repeated imaging and localization with high precision of single fluorophores within the sample. The final image can be rendered by plotting the position of each single emitter that can be precisely determined by measuring the center position of its image or PSF [61, 85]. As long as the number of photons

collected for each emitter (N) is sufficient, the fluorophore position is determined with precision higher than the diffraction limit (as schematically shown in Fig. 1a):

$$\sigma \sim \frac{s_0}{\sqrt{N}}$$

where σ is the localization precision, s_0 is the size of the PSF, and N is the number of photons/molecule.

Localization-based techniques allow imaging of sub-cellular structures with nanometer resolution and provide information at the molecular scale. Single-molecule imaging can be achieved exploiting the spectral properties of photoactivatable and photoswitchable proteins [56] or the transition to metastable dark states of conventional dyes [29, 33, 40]. So far, localization-based super-resolution methods are also robust enough for multicolor imaging of sub-cellular structures [3, 77, 84]. Now, the observation of structures with size beyond the diffraction limit requires an isotropic improvement in resolution, and this brought, in the last few years, to the development of 3D super-resolution strategies that allowed achieving single-molecule localization along the three dimensions. The implemented setup based on engineered PSF such as astigmatism [46], double-plane detection [48], interferometric approaches [78], and double helix PSF [53] clearly demonstrated 3D super-resolution imaging at the cell level. Notwithstanding this, imaging of the whole cells is still limited and suffers from extended excitation of out-of-focus signal regions. A strategy to alleviate this effect is represented by 2PE: temporal focusing approaches [90] allowed super-resolution imaging of protein distribution deep inside cells (10 μm). On the other side, the development of new class of fluorophores suitable for two-photon-induced molecular switching [32] allowed super-resolution with optical sectioning. More recently, 2PE and temporal focusing have been also used to confine the activation process in order to perform 3D super-resolution at the whole-cell level [98].

The application of localization-based methods to thick samples (>50 μm), such as tissues and organisms, often represents a challenge since it is limited by the high background, aberrations, and refractive index mismatch. Several approaches contribute to solve this problem, from the sample preparation to the development of new optical approaches and more robust localization algorithms. First, particular attention needs to be addressed to the sample preparation procedure in order to reduce refractive index mismatch and aberrations [46]. Recently, approaches based on single-molecule localization and array tomography, *tomo*STORM [63] allowed imaging of tissue samples with molecular resolution. Similarly, the use of near-infrared lasers enables multicolor super-resolution imaging of complex biological samples, such as cardiac tissue sections and neuronal hippocampal cultures [2]. Efforts have also been addressed to solve the practical problem represented by optical aberrations that distort the single-molecule images affecting the localization precision. To this end, optimal 3D localization methods, taking into account for optical system aberrations in case of arbitrary 3D PSFs in the presence of noise, have been recently presented in literature [68]. Furthermore, the out-of-focus

excitation and the high background can be alleviated by axially confining the excitation using an inclined illumination approach [87] or light-sheet-based microscopy [47] instead of a widefield illumination scheme.

Individual molecule localization combined with SPIM (IML-SPIM) has been recently applied to super-resolution imaging of thick mammary cell spheroids (up to 200 μm) [12, 13]. IML-SPIM allowed to reduce out-of-focus background signal and to observe the spatial distribution of connexin43 in selected regions of the cellular spheroid. The entire spheroid can be imaged by conventional SPIM (Fig. 1b) and 3D super-resolution images within a specific volume of interest can be performed at different depths (as represented in the color-coded map Fig. 1c). This approach, under two-photon photoactivation regime [74], has been further improved in terms of robustness to scattering artifacts [11–13, 52].

When dealing with thick scattering media, aberrations and light–sample interactions may decrease the SNR and thus the localization performances. Scattering effects and system instabilities can induce additional errors, and the localization precision can be redefined [1] by considering also the standard deviation σ_{inst} of the overall instabilities:

$$\sigma_{\text{eff}} = \sqrt{\sigma + \sigma_{\text{inst}}}$$

The real localization accuracy is strongly affected by low light conditions and background signal, and this effect is stronger when photons are collected deep within biological samples. When molecules are localized in depth within the sample, particular attention needs to be addressed to the real value of the effective accuracy [12, 13]. An experimental measure of its value can be directly obtained within the real sample by localizing point-like fluorescent objects in depth, both in the radial (63 nm) and axial (140 nm) direction, as shown in Fig. 1d and e, respectively. Similarly, a light-sheet-based approach has been used also for single particle tracking [80] deep within living tissue (up to 200 μm).

On the other side, the development of new robust algorithms for localization [81], able to localize molecule positions within high-density samples [62, 100] featuring high background regimes [79], represents a step forward super-resolution of more complicate and dense samples. In fact, an increasing number of new localization algorithms, based on gaussian fitting, MLE or compressed sensing have been developed to improve localization performances and temporal resolution and allowing single-molecule localization in highly dense samples. The synergy between the development of suitable optical architectures, new far-red or IR dyes and robust localization algorithms will smooth the way to super-resolution imaging of thicker samples or tissues [19].

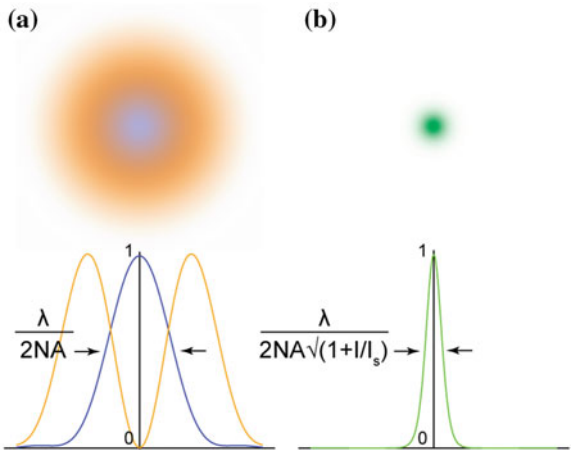

Fig. 2 The STED concept

4 Stimulated Emission Depletion (Sted-Like)

The first technique that made the diffraction barrier "crumbling" was STED microscopy [42]. In a STED microscope, a regularly focused excitation beam shared the focus with a second beam (usually called STED beam) able to de-excite the fluorophores via stimulated emission. Since the STED beam usually forms a doughnut shape, featuring a zero intensity in the center, all the fluorophores eventually located on the excitation spot are kept dark, except those in the proximity of the zero-intensity point, which, on the contrary, spontaneously emit, see Fig. 2. By increasing the intensity of the STED beam, the probability to de-excite the fluorescence via stimulated emission saturates at the outer part of the excitation spot, and the volume from which the fluorophores spontaneously emit decreases to sub-diffraction size. Scanning the two co-aligned beams across the sample and recording the spontaneously emitted fluorescence yield the final image whose spatial resolution can be tuned by the STED beam intensity.

Nevertheless, the spatial resolution of a STED system is theoretically "infinite"; many practical issues limit the ultimate value achievable. First, potential phototoxicity as well as photodamage effects on the sample limits the amount of STED light that is possible to imping. Second, many experimental imperfections in the focal intensity distributions of both STED and excitation beams, such as astigmatism, lateral misalignments, and zero-intensity point defects, reduce the contrast of the inhibition process, that is, so crucial obtaining substantial resolution improvement. The attainable resolution further reduces when imaging is performed depth into the sample, since to the experimental imperfections cited above, it is necessary adding scattering, absorption, and aberration induced by the sample itself.

An extreme way to circumvent the problem of depth imaging is to mimic the strategy adopted in electron microscopy: The sample is sectioned into a series of

thin slices, imaged on the microscope, and then dedicated software helps to merging all the slices into a three-dimensional structure. This method can greatly improve the performances of correlative light-electron microscopy [92]. Punge et al. [67] combined this method with STED and demonstrated 80 nm 3D spatial resolution in immunostained cultured rat hippocampal neurons. Under a complete different perspective, 2PE microscopy allows combining 3D non-invasive imaging capabilities with a reduced sensitivity to scattering effects, thus providing a golden standard for tissue imaging. Driven by these advantages, several groups [27, 39, 54, 59] have shown that 2PE can be realized within the STED microscopy umbrella, thus pushing the resolution of 2PE microscopy beyond the diffraction barrier. 2PE microscopy is usually performed with a high-repetition (80 MHz) train of ultrashort ($\sim$200-fs) laser pulses provided by mode-locked Ti:Sapphire lasers. The high concentration of photons in this short time ensures the TPE process takes place. In stark contrast, de-exciting fluorophores by stimulated emission is one-photon process, meaning that the STED beam can be supplied also by continuous-wave beams. In fact, the first combination of STED with two-photon microscopy was realized with continuous-wave STED beams [27, 59]. This combination greatly simplified the combination of 2PE and STED, because the depletion beam does not need to be synchronized with the ultrafast 2PE laser beam pulses. However, despite its simplicity, the classical CW-STED implementation is not able to provide the same imaging performance of the all-pulsed STED implementation [94]. It recently turned out that the development of gated CW-STED (gCW-STED) microscopy is able to provide further advances toward applications on living systems by allowing a significant reduction of the intensity needed by the depletion beam to get a certain super-resolution. gCW-STED essentially relies on a pulse de-excitation beam and time-gated detection [94]. An intuitive formulation to explain the principle governing the gCW-STED is that the stimulated emission (SE) shortens the average time that a fluorophore spends in the excited state, that is, its effective excited-state lifetime s varies inversely with the de-excitation rate of SE, which increases linearly with the STED beam intensity I_{STED} (Fig. 3a). Consequently, in the doughnut-shaped pattern, the excited-state lifetime of a fluorophore changes according to its position. In particular, the effective excited-state lifetime t decreases away from the zero-intensity point, reaching a minimum in the proximity of the doughnut crest where there is the maximum STED beam intensity $I^{\mathrm{m}}_{\mathrm{STED}}$ (Fig. 3b). By collecting the photons after a time delay T_{g} from the excitation events (time-gated detection) that are triggered by the pulses of the excitation beam, it is possible to reject photons emitted by short-lived, excited-state fluorophores, located in the periphery, and highlight photons emitted by long-lived excited-state fluorophores located close to the zero-intensity point. As a result, the effective area from which the fluorescence signal is registered is further confined (Fig. 3b). Theoretically, this area can be tuned to infinitely small size by infinitely delaying the detection, namely the full width at half-maximum of the effective fluorescent area scales as $d_c/\sqrt{\left(1+d_{\mathrm{c}}^2 a^2 I^{\mathrm{m}}_{\mathrm{STED}}/I_{\mathrm{sat}}\left(1+T_{\mathrm{g}}/(\mathrm{t_{fl}}\ln 2)\right)\right)}$, with d_{c} the effective area of the confocal associated confocal microscope, I_{sat} the intensity of the STED beam for which

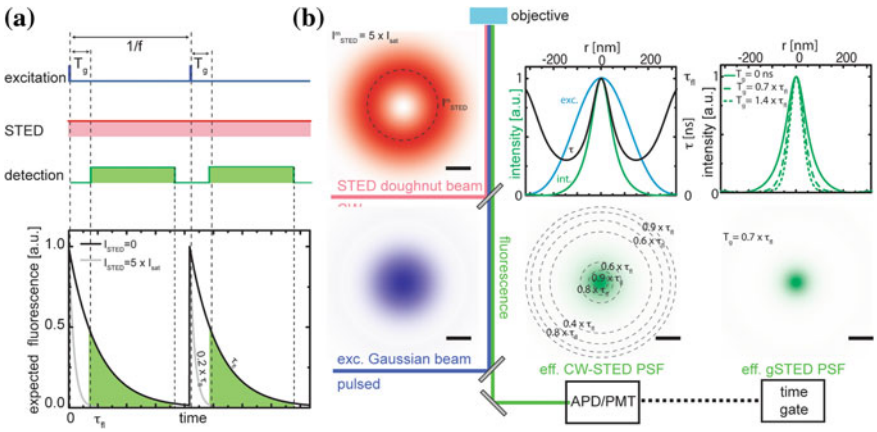

Fig. 3 Principles of gCW-STED microscopy. **a** Time evolution of the fluorescence signal in the absence ($I_{STED} = 0$) and presence ($I_{STED} = 5 \times I_{sat}$) of the STED beam with experimental time sequence (*upper panel*). **b** Schematic drawing of the gCW-STED setup with pulsed excitation (*blue*) and CW-STED (*red*) laser beams. Fluorescence light (*green*) is detected by the objective lens and imaged onto an avalanche photon detector (*APD*) or photomultiplier (*PMT*). A time-gating card discards the early photons (with respect to the excitation events). (**b**, *upper-left panel*) Calculated lateral intensity distribution for the excitation beam (*blue*), the effective region in which the dyes allow fluorescing (*green*) with the relative excite-state lifetime (*black*). (**b**, *lower-left panel*) The two-dimensional contour plot of the relative excite-state lifetime super-imposed with the two-dimensional effective fluorescence area. (**b**, *upper-right panel*) Calculated lateral intensity distribution for the gCW-STED effective point spread function for increasing time delay T_g of the gated detection. (**b**, *lower-right panel*) The two-dimensional effective point spread function. Scale bars 100 nm

the probability of spontaneous emission equals the probability of stimulated emission, t_{fl} the excited-state lifetime of the unperturbed fluorophore, and a a constant that depends on the doughnut shape of the STED beam. However, the loss of signal, which is intrinsic to the gated detection, fixes an upper limit on the time delay [91].

Two further approaches have been implemented to improve the 2PE-STED performances in depth. A first method has been recently realized by two groups [5, 54, 82], which have simultaneously elaborated an all-pulsed 2PE-STED implementation based on the synchronization of two femtosecond mode-locked Ti:Sapphire lasers, see Fig. 4.

Another effective method performs 2PE-STED imaging using a single wavelength (SW) for 2PE and depletion [39]. The related SW 2PE-STED setup simplifies the image formation scheme, provides the super-resolution advantage of a pulsed STED, and allows maintaining a comparatively low cost, see Fig. 5.

It is worth noting that even if the stimulated emission process is a one-photon process, scattering of stimulating photons will not represent a source of background since, in most of the case, their wavelength is far away from the absorption

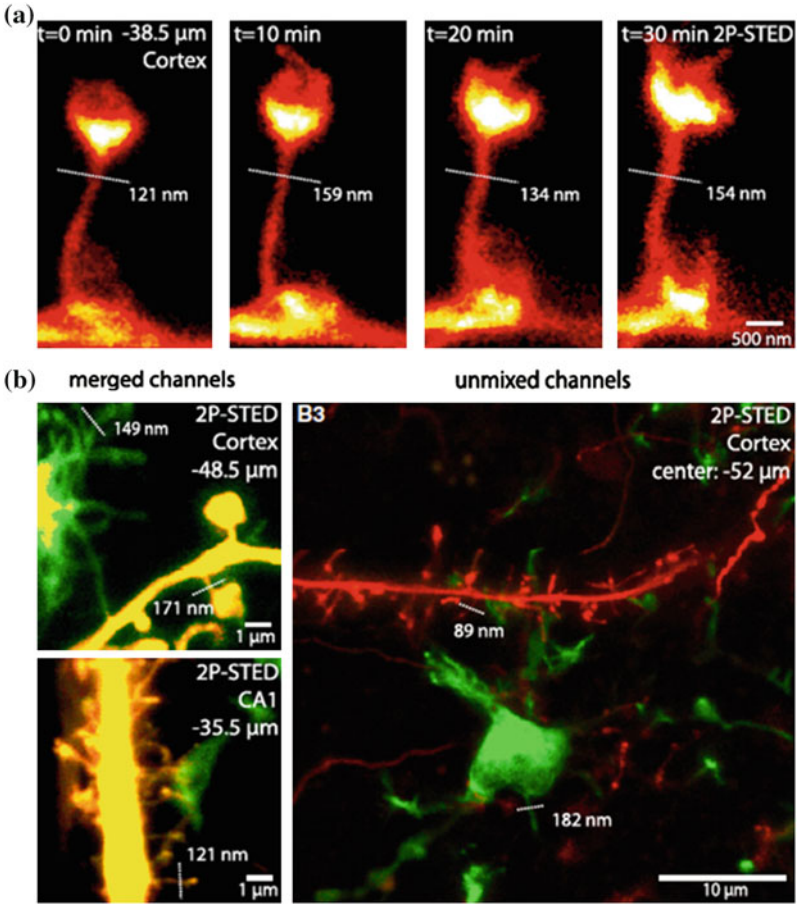

Fig. 4 Time-lapse and dual-color 2P-STED imaging. **a** Time-lapse images of a cortical spine acquired at 38.5 µm below the tissue surface. **b** Two-color 2PE-STED imaging of neurons and microglia (from [5])

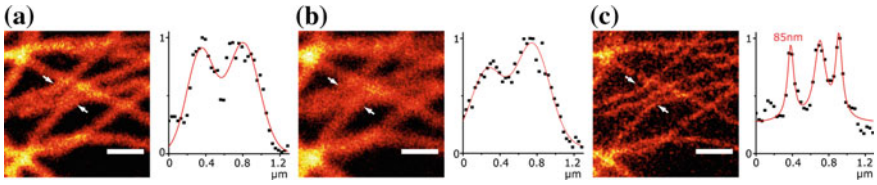

Fig. 5 Immunofluorescence 2PE-STED single-wavelength microscopy shown in comparison with confocal and 2PE microscopy (**a**–**c**). **a** Confocal (excitation at 633 nm), **b** 2PE (excitation at 770 nm), and **c** 2PE-STED (excitation and depletion at 770 nm) micrographs of microtubules immunostained with the dye ATTO647N. On the right of each image, we plotted the line profile (*black squares*) along the *arrows* indicated in the images, together with a multiple peak fit (*red*). (Scale bars: 1 µm). Modified from (Bianchini, Harke et al. 2012)

spectral window of the dye and in the worst scenario, fluorescence signal induced by the STED beam can be subtracted by lock-in technique [69, 93]. On the contrary, the major problem appears when due to scattering and due to aberration the stimulating photons destroy the quality of the zero-intensity point. In this scenario, stimulated depletion occurs also in the region from which one wants to collect fluorescence and the spatial resolution fast degrade [34]. Two elegant methods have been combined with STED microscopy for compensating the aberrations induced on the STED intensity distribution when imaging is performed deep into sample. Notably, both methods have been demonstrated in the one-photon excitation regime; however, combination with TPE could in principle be reliable. A possibility of improvement is given by the development of new aberration-reducing objective lenses for fluorescence microscopy. By adjusting the correction collar of the objective lenses and carefully choosing the refractive index of the objective embedding medium, Urban and colleagues [89] resolved distinct distribution of actin inside dendrites and spines with a resolution of 60–80 nm in living organotypic brain slices at depths up to 120 μm. Also, adaptive optics can be utilized to compensate for aberration in STED microscopy, which uses adaptive optics. Gould et al. [35] showed that using spatial light modulators both in the excitation and STED beam can substantially compensate sample-induced aberration in a three-dimensional STED implementation. It is worth noting that the SW-2PE-STED approach can improve the above-mentioned situations depending on the availability of suitable fluorescent molecules [39].

5 Perspective Note

Despite the fact that so-called super-resolution methods can be still considered in their infacy, so many technical variations have been implemented that is quite impossible to mention all of them. It is self-evident how targeted and stochastic methods tend to merge their own “technicalities.” We think that two emerging classes of new approaches could be very promising, namely smart investigation of the sample toward 3D super-resolution in thick scattering specimens [25, 28] and coupling with scanning probe methods extending the domain of correlative microscopy to atomic force microscopy [14, 15, 28, 39, 60]. Also, further advances in optical super-resolution methods are the ones related to the exploitation of parameters such as phase, polarization, and absorption, also moving the investigation regime from visible radiation to the infrared one.

References

1. Aquino D, Schönle A, Geisler C, Middendorff CV, Wurm CA, Okamura Y, Lang T, Hell SW, Egner A (2011) Two-color nanoscopy of three-dimensional volumes by 4Pi detection of stochastically switched fluorophores. Nat Methods 8(4):353–359
2. Baddeley D, Crossman D, Rossberger S, Cheyne JE, Montgomery JM, Jayasinghe ID, Cremer C, Cannell MB, Soeller C (2011) 4D super-resolution microscopy with conventional fluorophores and single wavelength excitation in optically thick cells and tissues. PLoS One 6(5):e20645
3. Bates M, Huang GTDB, Zhuang X (2007) Multicolor super-resolution imaging with photo-switchable fluorescent probes. Science 317:1749–1753
4. Berning S, Willig KI, Steffens H, Dibaj P, Hell SW (2012) Nanoscopy in a living mouse brain. Science 335(6068):551
5. Bethge P, Chéreau R, Avignone E, Marsicano G, Nägerl UV (2013) Two-photon excitation STED microscopy in two colors in acute brain slices. Biophys J 104(4):778–785
6. Betzig E, Chichester RJ (1993) Single molecules observed by near field scanning optical microscopy. Science 262:1422–1425
7. Betzig E, Patterson GH, Sougrat R, Lindwasser OW, Olenych S, Bonifacino JS, Davidson MW, Lippincott-Schwartz J, Hess HF (2006) Imaging intracellular fluorescent proteins at nanometer resolution. Science 313(5793):1642–1645
8. Bianchini P, Harke B, Galiani S, Vicidomini G, Diaspro A (2012) Single-wavelength two-photon excitation-stimulated emission depletion (SW2PE-STED) superresolution imaging. Proc Natl Acad Sci USA 109(17): 6390–6393
9. Bianco B, Diaspro A (1989) Analysis of the three dimensional cell imaging obtained with optical microscopy techniques based on defocusing. Cell Biophys 15(3):189–200
10. Bobroff N (1986) Position measurement with a resolution and noise limited instrument. Rev Sci Instrum 57(6):1152–1157
11. Cella Zanacchi F, Lavagnino Z, Faretta M, Furia L, Diaspro A (2013) Light-sheet confined super-resolution using two-photon photoactivation. PLoS One 8(7):e67667
12. Cella Zanacchi F, Lavagnino Z, Perrone Donnorso M, Del Bue A, Furia L, Faretta M, Diaspro A (2011) Live-cell 3D super-resolution imaging in thick biological samples. Nat Methods 8(12):1047–1049
13. Cella Zanacchi F, Lavagnino Z, Ronzitti E, Diaspro A (2011) Two-photon fluorescence excitation within a light sheet based microscopy architecture. Proc SPIE 7903(1)
14. Chacko JV, Canale C, Harke B, Diaspro A (2013) Sub-diffraction nano manipulation using STED AFM. PLoS One 8(6):e66608
15. Chacko JV, Zanacchi FC, Diaspro A (2013) Probing cytoskeletal structures by coupling optical superresolution and AFM techniques for a correlative approach. Cytoskeleton 70(11):729–740
16. Chirico G, Cannone F, Beretta S, Baldini G, Diaspro A (2001) Single molecule studies by means of the two-photon fluorescence distribution. Microsc Res Tech 55(5):359–364
17. Chirico G, Cannone F, Beretta S, Diaspro A, Campanini B, Bettati S, Ruotolo R, Mozzarelli A (2002) Dynamics of green fluorescent protein mutant2 in solution, on spin-coated glasses, and encapsulated in wet silica gels. Protein Sci 11(5):1152–1161
18. Coelho M, Maghelli N, Tolic-Norrelykke IM (2013) Single-molecule imaging in vivo: the dancing building blocks of the cell. Integr Biol (Camb) 5(5):748–758
19. Del Bue A, Cella Zanacchi F, Diaspro A (2013). Super-resolution 3D reconstruction of thick biological samples: a computer vision perspective. IEEE international conference on computer vision (ICCV)
20. Denk W, Strickler JK, Webb WW (1990) Two photon laser scanning fluorescence microscopy. Science 248(4951):73–76
21. Denk W, Svoboda K (1997) Photon upmanship: why multiphoton imaging is more than a gimmick. Neuron 18(3):351–357

22. Diaspro A (2001) Confocal and two-photon microscoscopy: foundations, applications, and advances. Wiley-Liss Inc, New York
23. Diaspro A (2010a) Nanoscopy and multidimensional optical fluorescence microscopy. CRC Press, Taylor & Francis
24. Diaspro A (2010b) Optical fluorescence microscopy: from the spectral to the nano dimension. Springer, Berlin
25. Diaspro A (2013) Taking three-dimensional two-photon excitation microscopy further: encoding the light for decoding the brain. Microsc Res Tech 76(10):985–987
26. Diaspro A, Chirico G, Collini M (2006) Two-photon fluorescence excitation and related techniques in biological microscopy. Q Rev Biophys 15:1–70
27. Ding JB, Takasaki KT, Sabatini BL (2009) Supraresolution imaging in brain slices using stimulated-emission depletion two-photon laser scanning microscopy. Neuron 63(4): 429–437
28. Ducros M, Houssen YG, Bradley J, de Sars V, Charpak S (2013) Encoded multisite two-photon microscopy. Proc Natl Acad Sci USA 110(32):13138–13143
29. Egner A, Geisler C, von Middendorff C, Bock H, Wenzel D, Medda R, Andresen M, Stiel AC, Jakobs S, Eggeling C, Schönle A, Hell SW (2007) Fluorescence nanoscopy in whole cells by asynchronous localization of photoswitching emitters. Biophys J 93(9):3285–3290
30. Fernandez-Suarez M, Ting AY (2008) Fluorescent probes for super-resolution imaging in living cells. Nat Rev Mol Cell Biol 9(12):929–943
31. Flors C (2013) Super-resolution fluorescence imaging of directly labelled DNA: from microscopy standards to living cells. J Microsc 251(1):1–4
32. Fölling J, Belov V, Riedel D, Schönle A, Egner A, Eggeling C, Bossi M, Hell SW (2008) Fluorescence nanoscopy with optical sectioning by two-photon induced molecular switching using continuous-wave lasers. ChemPhysChem 9(2):321–326
33. Fölling J, Bossi M, Bock H, Medda R, Wurm CA, Hein B, Jakobs S, Eggeling C, Hell SW (2008) Fluorescence nanoscopy by ground-state depletion and single-molecule return. Nat Methods 5(11):943–945
34. Galiani S, Harke B, Vicidomini G, Lignani G, Benfenati F, Diaspro A, Bianchini P (2012) Strategies to maximize the performance of a STED microscope. Opt Express 20(7):7362–7374
35. Gould TJ, Burke D, Bewersdorf J, Booth MJ (2012) Adaptive optics enables 3D STED microscopy in aberrating specimens. Opt Express 20(19):20998–21009
36. Gustafsson MG (2000) Surpassing the lateral resolution limit by a factor of two using structured illumination microscopy. J Microsc 198(Pt 2):82–87
37. Gustafsson MG (2005) Nonlinear structured-illumination microscopy: wide-field fluorescence imaging with theoretically unlimited resolution. Proc Natl Acad Sci USA 102:13081–13086
38. Gustafsson MG, Shao L, Carlton PM, Wang CJR, Golubovskaya IN, Cande WZ, Agard DA, Sedat JW (2008) Three-dimensional resolution doubling in wide-field fluorescence microscopy by structured illumination. Biophys J 94(12):4957–4970
39. Harke B, Chacko JV, Haschke H, Canale C, Diaspro A (2012) A novel nanoscopic tool by combining AFM with STED microscopy. Opt Nanoscopy 1(1):3
40. Heilemann M, van de Linde S, Mukherjee A, Sauer M (2009) Super-resolution imaging with small organic fluorophores. Angew Chem Int Ed Engl 48(37):6903–6908
41. Hell SW (2007) Far-field optical nanoscopy. Science 316(5828):1153–1158
42. Hell SW, Wichmann J (1994) Breaking the diffraction resolution limit by stimulated emission: stimulated-emission-depletion fluorescence microscopy. Opt Lett 19(11):780–782
43. Hess ST, Girirajan TPK, Mason MD (2006) Ultra-high resolution imaging by fluorescence photoactivation localization microscopy. Biophys J 91(11):4258–4272
44. Hou S, Liang L, Deng S, Chen J, Huang Q, Cheng Y, Fan C (2013) Nanoprobes for super-resolution fluorescence imaging at the nanoscale. Sci China Chem 57(1):100–106
45. Huang B (2011) An in-depth view. Nat Methods 8(4):304–305

46. Huang B, Jones SA, Brandenburg B, Zhuang X (2008) Whole-cell 3D STORM reveals interactions between cellular structures with nanometer-scale resolution. Nat Methods 5(12):1047–1052
47. Huisken J, Swoger J, Bene FD, Wittbrodt J, Stelzer EHK (2004) Optical sectioning deep inside live embryos by selective plane illumination microscopy. Science 305(5686): 1007–1009
48. Juette MF, Gould TJ, Lessard MD, Mlodzianoski MJ, Nagpure BS, Bennett BT, Hess ST, Bewersdorf J (2008) Three-dimensional sub-100 nm resolution fluorescence microscopy of thick samples. Nat Methods 5(6):527–529
49. Keller PJ, Schmidt AD, Wittbrodt J, Stelzer EHK (2008) Reconstruction of zebrafish early embryonic development by scanned light sheet microscopy. Science 322(5904):1065–1069
50. Kempf C, Staudt T, Bingen P, Horstmann H, Engelhardt J, Hell SW, Kuner T (2013) Tissue multicolor STED nanoscopy of presynaptic proteins in the calyx of held. PLoS One 8(4):e62893
51. Kim H, Ha T (2013) Single-molecule nanometry for biological physics. Rep Prog Phys 76:1–16
52. Lavagnino Z, Cella Zanacchi F, Ronzitti E, Diaspro A (2013) Two-photon excitation selective plane illumination microscopy (2PE-SPIM) of highly scattering samples: characterization and application. Opt Express 21(5):5998–6008
53. Lee H-LD, Sahl SJ, Lew MD, Moerner WE (2012) The double-helix microscope super-resolves extended biological structures by localizing single blinking molecules in three dimensions with nanoscale precision. Appl Phys Lett 100(15):153701–1537013
54. Li Q, Wu SSH, Chou KC (2009) Subdiffraction-limit two-photon fluorescence microscopy for GFP-tagged cell imaging. Biophys J 97(12):3224–3228
55. Loew LM, Hell SW (2013) Superresolving dendritic spines. Biophys J 104(4):741–743
56. Lukyanov KA, Chudakov DM, Lukyanov S, Vverkhusha V (2005) Innovation: photoactivatable fluorescent proteins. Nat Rev Mol Cell Biol 6(11):885–889
57. Mandula O, Wicker MKK, Krampert G, Kleppe I, Heintzmann R (2012) Line scan: structured illumination microscopy super-resolution imaging in thick fluorescent samples. Opt Express 20:24167–24174
58. Moerner WE, Kador L (1989) Optical detection and spectroscopy of single molecules in a solid. Phys Rev Lett 62:2535–2538
59. Moneron G, Hell SW (2009) Two-photon excitation STED microscopy. Opt Express 17(17):14567–14573
60. Monserrate A, Casado S, Flors C (2013) Correlative atomic force microscopy and localizationbased superresolution microscopy: revealing labelling and image reconstruction artefacts. ChemPhysChem Comm, pp 1–5 (in press)
61. Mortensen KI, Churchman LS, Spudich JA, Flyvbjerg H (2010) Optimized localization analysis for single-molecule tracking and super-resolution microscopy. Nat Methods 7(5):377–381
62. Mukamel EA, Babcock H, Zhuang X (2012) Statistical deconvolution for superresolution fluorescence microscopy. Biophys J 102(10):2391–2400
63. Nanguneri S, Flottmann B, Horstmann H, Heilemann M, Kuner T (2012) Three-dimensional, tomographic super-resolution fluorescence imaging of serially sectioned thick samples. PLoS One 7(5):e38098
64. Ntziachristos V (2010) Going deeper than microscopy: the optical imaging frontier in biology. Nat Methods 7(8):603–614
65. Palero J, Santos SICO, Artigas D, Loza-Alvarez P (2010) A simple scanless two-photon fluorescence microscope using selective plane illumination. Opt Express 18(8):8491–8498
66. Pawley J (Ed.) (2006) Handbook of biological confocal microscopy, 3rd ed., XXVIII, p 988 Springer
67. Punge A, Rizzoli SO, Jahn R, Wildanger JD, Meyer L, SchÃnle A, Kastrup L, Hell SW (2008) 3D reconstruction of high-resolution STED microscope images. Microsc Res Tech 71(9):644–650

68. Quirin S, Pavani SRP, Piestun R (2012) Optimal 3D single-molecule localization for superresolution microscopy with aberrations and engineered point spread functions. Proc Natl Acad Sci USA 109(3):675–679
69. Ronzitti E, Harke B, Diaspro A (2013) Frequency dependent detection in a STED microscope using modulated excitation light. Opt Express 21(1):210–219
70. Rust MJ, Bates M, Zhuang X (2006) Sub-diffraction-limit imaging by stochastic optical reconstruction microscopy (STORM). Nat Methods 3(10):793–795
71. Sahl SJ, Moerner WE (2013) Super-resolution fluorescence imaging with single molecules. Curr Opin Struct Biol 23(5):778–787
72. Schermelleh L, Carlton PM, Haase S, Shao L, Winoto L, Kner P, Burke B, Cardoso MC, Agard DA, Gustafsson MGL, Leonhardt H, Sedat JW (2008) Subdiffraction multicolor imaging of the nuclear periphery with 3D structured illumination microscopy. Science 320(5881):1332–1336
73. Schermelleh L, Heintzmann R, Leonhardt H (2010) A guide to super-resolution fluorescence microscopy. J Cell Biol 190(2):165–175
74. Schneider M, Barozzi S, Testa I, Faretta M, Diaspro A (2005) Two-photon activation and excitation properties of PA-GFP in the 720-920-nm region. Biophys J 89(2):1346–1352
75. Shao L, Kner P, Rego EH, Gustafsson MGL (2011) Super-resolution 3D microscopy of live whole cells using structured illumination. Nat Methods 8(12):1044–1046
76. Sheppard CRJ (2002) The generalized microscope. In: Diaspro A (ed) Confocal and two-photon microscopy: foundations, applications and advances. Wiley-Liss, New York, pp 1–18
77. Shroff H, Galbraith CG, Galbraith JA, White H, Gillette J, Olenych S, Davidson MW, Betzig E (2007) Dual-color superresolution imaging of genetically expressed probes within individual adhesion complexes. Proc Natl Acad Sci USA 104(51):20308–20313
78. Shtengel G, Galbraith JA, Galbraith CG, Lippincott-Schwartz J, Gillette JM, Manley S, Sougrat R, Waterman CM, Kanchanawong P, Davidson MW, Fetter RD, Hess HF (2009) Interferometric fluorescent super-resolution microscopy resolves 3D cellular ultrastructure. Proc Natl Acad Sci USA 106(9):3125–3130
79. Smith CS, Joseph N, Rieger B, Lidke KA (2010) Fast, single-molecule localization that achieves theoretically minimum uncertainty. Nat Methods 7(5):373–375
80. Spille J-H, Kaminski T, Königshoven H-P, Kubitscheck U (2012) Dynamic three-dimensional tracking of single fluorescent nanoparticles deep inside living tissue. Opt Express 20(18):19697–19707
81. Starr R, Stahlheber S, Small A (2012) Fast maximum likelihood algorithm for localization of fluorescent molecules. Opt Lett 37(3):413–415
82. Takasaki KT, Ding JB, Sabatini BL (2013) Live-cell superresolution imaging by pulsed STED two-photon excitation microscopy. Biophys J 104(4):770–777
83. Testa I, Urban NT, Jakobs S, Eggeling C, Willig KI, Hell SW (2012) Nanoscopy of living brain slices with low light levels. Neuron 75(6):992–1000
84. Testa I, Wurm CA, Medda R, Rothermel E, von Middendorf C, Fölling J, Jakobs S, Schönle A, Hell SW, Eggeling C (2010) Multicolor fluorescence nanoscopy in fixed and living cells by exciting conventional fluorophores with a single wavelength. Biophys J 99(8):2686–2694
85. Thompson RE, Larson DR, Webb WW (2002) Precise nanometer localization analysis for individual fluorescent probes. Biophys J 82(5):2775–2783
86. Tinoco I Jr, Gonzalez RL Jr (2011) Biological mechanisms, one molecule at a time. Genes Dev 25(12):1205–1231
87. Tokunaga M, Imamoto N, Sakata-Sogawa K (2008) Highly inclined thin illumination enables clear single-molecule imaging in cells. Nat Methods 5(2):159–161
88. Truong TV, Supatto W, Koos DS, Choi JM, Fraser SE (2011) Deep and fast live imaging with two-photon scanned light-sheet microscopy. Nat Methods 8(9):757–760
89. Urban NT, Willig KI, Hell SW, Nagerl UV (2011) STED nanoscopy of actin dynamics in synapses deep inside living brain slices. Biophys J 101(5):1277–1284

90. Vaziri A, Tang J, Shroff H, Shank CV (2008) Multilayer three-dimensional super resolution imaging of thick biological samples. Proc Natl Acad Sci USA 105(51):20221–20226
91. Vicidomini G, Coto Hernandez I, d'Amora M, Cella Zanacchi F, Bianchini P, Diaspro A (2013) Gated CW-STED microscopy: a versatile tool for biological nanometer scale investigation. Methods
92. Vicidomini G, Gagliani MC, Cortese K, Krieger J, Buescher P, Bianchini P, Boccacci P, Tacchetti C, Diaspro A (2010) A novel approach for correlative light electron microscopy analysis. Microsc Res Tech 73(3):215–224
93. Vicidomini G, Moneron G, Eggeling C, Rittweger E, Hell SW (2012) STED with wavelengths closer to the emission maximum. Opt Express 20(5):5225–5236
94. Vicidomini G, Moneron G, Han KY, Westphal V, Ta H, Reuss M, Engelhardt J, Eggeling C, Hell SW (2011) Sharper low-power STED nanoscopy by time gating. Nat Methods 8(7):571–575
95. Wilson T, Sheppard CJR (1984) Theory and practice of scanning optical microscopy. Academic Press, Waltham
96. Xie XS (1996) Single-molecule spectroscopy and dynamics at room temperature. Acc Chem Res 29:598–606
97. Yildiz A, Selvin PR (2005) Fluorescence imaging with one nanometer accuracy: application to molecular motors. Acc Chem Res 38(7):574–582
98. York AG, Ghitani A, Vaziri A, Davidson MW, Shroff H (2011) Confined activation and subdiffractive localization enables whole-cell PALM with genetically expressed probes. Nat Methods 8(4):327–333
99. York AG, Parekh SH, Nogare DD, Fischer RS, Temprine K, Mione M, Chitnis AB, Combs CA, Shroff H (2012) Resolution doubling in live, multicellular organisms via multifocal structured illumination microscopy. Nat Methods 9(7):749–754
100. Zhu L, Zhang W, Elnatan D, Huang B (2012) Faster STORM using compressed sensing. Nat Methods 9(7):721–723